J. Fluid Mech. (1986), *vol.* 172, 1–15
Printed in Great Britain

Vortex pairs and rings interacting with shear-layer vortices

By M. KIYA, M. OHYAMA
Faculty of Engineering, Hokkaido University, Sapporo, 060, Japan

AND J. C. R. HUNT
Department of Applied Mathematics and Theoretical Physics,
University of Cambridge, Cambridge, UK

(Received 14 January 1985 and in revised form 22 January 1986)

In order to understand how free-stream turbulence affects the vortex-pairing mechanism in free-mixing layers, water-flume experiments have been performed on the interaction between single vortex pairs (with circulation Γ_{vp}) and also vortex rings propelled towards the rolling-up vortices (of circulation Γ_{sh}) in a two-dimensional separated shear layer. The Reynolds number of an obstacle generating the shear layer is about 10^3 and of the vortex pairs and rings about 10–100. Our observations show that, if the ratio Γ_{vp}/Γ_{sh} exceeds about 1.4, the vortex pairs break away any shear-layer vortices in their path and if Γ_{vp}/Γ_{sh} is less than about 0.5 the shear-layer vortices destroy the vortex pair. But if $\Gamma_{vp}/\Gamma_{sh} = 1.0 \pm 0.4$ the vortex pairs and shed vortices interact strongly, for example by a pairing between one vortex of the pair and the shed vortex, by the vortex pair eliminating coalescence of vortices in the shear layer, or by combining with the rolling-up vortices to generate large vortices. Qualitatively similar effects are observed with the vortex rings.

Numerical calculations of the interaction between an array of vortices on a line and a vortex pair are described. The results are similar to those of the physical experiments, in particular displaying the same sensitivity to Γ_{vp}/Γ_{sh} at $\Gamma_{vp}/\Gamma_{sh} \approx 1.0$. It is suggested that these results demonstrate one important way in which free-stream turbulence interacts with shear layers and how shear layers interact with other vortices.

1. Introduction

Turbulent shear layers frequently occur in a free stream with turbulence. The effect of the free-stream turbulence on shear layers has been studied by many authors; see, among others, Bradshaw (1974), Hancock & Bradshaw (1983), Castro (1984) for turbulent boundary layers and Symes & Fink (1977), Chandrsuda *et al.* (1978), Pui & Gartshore (1979), Wygnanski *et al.* (1979), Oguchi & Inoue (1984) for free turbulent shear layers. These studies discuss global features of shear layers such as the growth rate, lateral profiles of the time-mean and fluctuating velocities, etc. in terms of the lengthscale and intensity of the free-stream turbulence.

The present paper has resulted from an attempt to understand the free-stream turbulence effects in terms of direct interaction between large-scale coherent vortices in shear layers and energy-containing vortices in the free stream. We consider that a first step to this goal is to study single vortices interacting with the vortices of the shear layers. In what follows, the coherent vortices will be referred to as shear-layer vortices and the vortices in the free stream as external vortices.

We consider a plane mixing layer between a uniform stream and a still fluid. At a sufficiently high Reynolds number, the mixing layer rolls-up to form concentrated vortices. These shear-layer vortices are the dominant source of velocity fluctuations in the layer. There is now substantial experimental evidence that the shear-layer vortices are fairly two-dimensional even in the fully developed region (e.g. Oguchi & Inoue 1984).

We presume that the shear-layer vortices are most strongly affected by external vortices of the same lengthscale. External vortices much larger than the shear-layer vortices produce a lateral flapping of the mixing layer without changing the inherent structure of the shear-layer vortices (Bradshaw 1977). On the other hand, external vortices much smaller than the shear-layer vortices are expected to behave rather passively near a shear-layer vortex. Moreover, in general the vortices in a mixing layer are much stronger than most vortices likely to be found in the free stream. Accordingly we consider external vortices whose lengthscale is of the same order as that of the shear-layer vortices and of strength of the same order as or less than that of the shear-layer vortices.

Single rectilinear vortex pairs and single vortex rings were chosen in this study as a model of external vortices, a choice justified by the fact that turbulent shear layers consist of structures that look like vortex pairs, rings and lines as demonstrated by Falco (1977), Perry & Lim (1978), Head & Bandyopadhyay (1983), among others. As a first step to understand the complicated patterns of the interaction, we chose vortex pairs with their axis parallel to that of the shear-layer vortices and vortex rings moving in a plane normal to these axes.

Experimental works on vortex interactions are rather scarce: Yamada & Matsui (1979) for the interaction between vortex rings, and Tatsuno & Honji (1977) for that between vortex pairs. Theoretical works on the interaction between multiple rectilinear vortices are reviewed by Aref (1983) with an extensive list of references. Motion and deformation of multiple finite-area vortex regions are considered via the contour dynamics by Zabusky, Hughes & Roberts (1979) and Overman & Zabusky (1982). These papers, however, give only limited information on the interaction between a vortex pair and shear-layer vortices.

2. Experimental apparatus and method

2.1. *The experiment with vortex pairs*

The experiment was performed in an open-return water channel with a 15 cm high, 30 cm wide and 127 cm long working section (installed in the Department of Mechanical Engineering, Hokkaido University). A three-stage honeycomb was placed in a calming chamber upstream of the test section. The channel was filled with tap water to a depth of 13 cm in the test section.

The time-mean longitudinal velocity was measured by time lines of hydrogen bubbles or by a small propeller velocimeter at various spanwise and longitudinal positions. The velocity profile in the test section was found to be fairly uniform in a region ± 2.5 cm centred around the mid-depth. The r.m.s. longitudinal velocity measured by a constant-temperature hot-film velocimeter was 0.5% along the centreline of the test section. Other details of the channel are given in Tamura, Kiya & Arie (1984).

A shear layer was produced by the separation from a sharp edge of a thin plate attached normally to a smooth flat sidewall of the test section. The plate was 4.3 cm high, 1.0 cm thick and had a span of 15 cm. Its edge was bevelled downstream with

an angle of 45°, the bevelled side being about 1.4 cm. The plate thus had an aspect ratio of 3.5 and its blockage of the test section amounted to 14.3%. The bevelled side of the plate had a hole 1 mm in diameter at 5.5 mm downstream of the edge to supply (red) dye for visualization of the shear layer. The dye was continuously introduced into the flow, with a very small velocity, from an outside reservoir through the interior of the plate.

The dye moved towards the edge in a reverse flow and eventually entrained into the shear layer. The dye thus gives a streakline approximately coinciding with the centreline of the shear layer. A flow-visualization study using hydrogen bubbles showed that the shear layer was almost parallel to the spanwise direction over about 5 cm ($= 1.16h$) centred around the mid-span.

A large recirculating region was formed behind the plate. The recirculating flow usually contains high turbulence, so that we expect it to affect the rolling-up of the shear layer near the plate (Chandrsuda *et al.* 1978). This point will be discussed later.

The strength of the shear-layer vortices was changed by adjusting the free-stream velocity U_∞ in the range 1.6–2.8 cm/s. The Reynolds number Re based on U_∞ and the plate height h ranged from 690 to 1200.

We shall now estimate to what extent the dye represents the diffusion of vorticity in the shear layer. The lateral extent of the distributed vorticity in the shear layer is given by the maximum-slope thickness b (see, for example, Winant & Browand 1974). For a steady plane (laminar) mixing layer

$$\frac{b}{h} = 5.1(Re)^{-\frac{1}{2}}\left(\frac{x}{h}\right)^{-\frac{1}{2}},$$

where x is the longitudinal distance measured from the edge of the plate (Batchelor 1967). For a Reynolds number $Re = 1000\,b/h = 0.16$ or $b = 5$ mm at $x/h = 1.0$. This is much greater than the thickness of the dye filament at the same longitudinal position, as seen in figure 3; that is the vorticity diffuses beyond the region occupied by the dye. It should be noted, however, that the vorticity probably attains a local maximum at the centre of the dye filament because the vorticity was mostly concentrated in the dye at the separation edge. Accordingly a region where the dye filament exhibits a vortex-like structure perhaps has larger vorticity than its surroundings. In this paper such a region is interpreted as a shear-layer vortex.

A two-dimensional nozzle, illustrated in figure 1, was used to produce a vortex pair. The nozzle was 4.5 mm wide, protruding 3.0 cm from the sidewall; the centre of the nozzle was 3.25 cm downstream of the front face of the plate. The vortex pair was ejected from the low-velocity side to the high-velocity side of the shear layer.

Single vortex pairs were produced by suddenly pouring a small amount of water from outside into a reservoir connected to the nozzle (see figure 1). Its strength was controlled by adjusting the amount of poured water, which was 10–25 cm^3, and this was poured in about 0.5 s. The vortex pair was visualized by (blue) fine particles produced from solid ink flush-mounted onto the inside of the nozzle.

The width of the nozzle was chosen so that the distance between the pair of vortices was of the same order as that of the shear-layer vortices when the interactions started. The vortex pair travelled about 5 cm before its destruction by a spanwise instability which caused the vortex pair to roll-up to form a few vortex rings (Crow 1970), as shown in figure 2. This distance was only weakly dependent on the strength of the vortex pair. Moreover, the height of protrusion of the nozzle (3.0 cm) was chosen so that the vortex pair started to interact with the shear-layer vortices well before it had travelled the 5 cm.

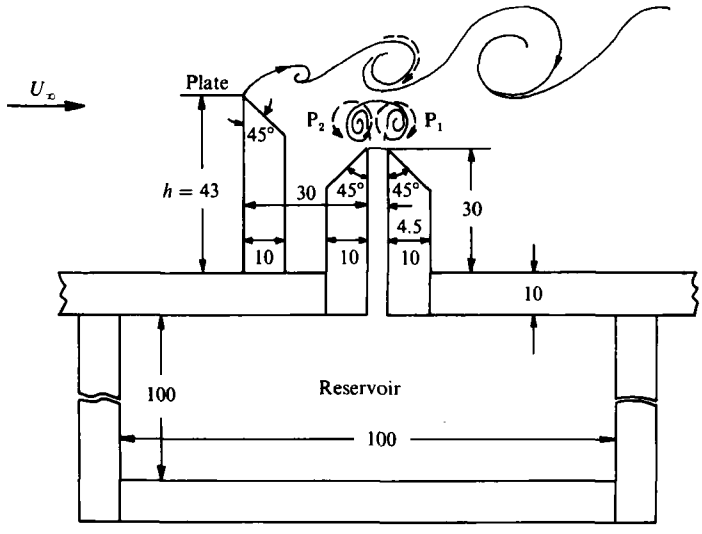

FIGURE 1. Nozzle and normal plate for generating single vortex pairs and a separated shear layer respectively. P_1 and P_2 are pair vortices. Flow is from left to right. Dimensions in mm.

The nozzle possibly influences the rolling-up of the shear layer because it protrudes into the vicinity of the shear layer. Some effect of the turbulence transported by the recirculating flow is also expected. Thus patterns of the shear-layer vortices such as shown in figure 3 should be considered as having been influenced by the two agents. This is immaterial, however, to the present study because such shear-layer vortices can still give essential information on the interaction between shear-layer vortices and external vortices. On the other hand, the motion of the vortices was seen to be influenced by the nozzle when they came close to it. Accordingly most of the discussion in §4 is confined to a period in which the vortices were sufficiently far from the nozzle. Various patterns of the interaction were recorded by a video camera and later observed on a videoscreen. Photographs were taken from the videoscreen.

2.2. *The experiment with a vortex ring*

This experiment was performed in an open-return recirculating water channel installed in the Hydraulic Laboratory, Department of Engineering, The University of Cambridge, England. The test section of the channel had a 10 cm × 10 cm cross-section and a length of 76 cm. The flow in the channel was produced by means of a multiple-disk pump, which was constructed from the design of Odell & Kovasznay (1971); details of the flow in the channel is given by Brighton (1977).

Shear-layer vortices were produced by the separation from a 'plate' attached normally to a sidewall of the test section. The 'plate' was actually a prism of an isosceles triangle cross-section which spanned the whole height of the sidwall; the longest side was set normal to the main stream; the maximum thickness normal to this side was approximately 1.0 cm.

A special feature of this experiment is that the fluid in the channel is stratified with a stable density gradient. Without this a considerable spanwise motion was observed in the shear layer owing to poor uniformity of flow in the test section. The density stratification was introduced to suppress this motion and thus to facilitate the flow visualization. We presume that, despite the density stratification, the main features of the deformation in the plane of the flow associated with the interaction are still

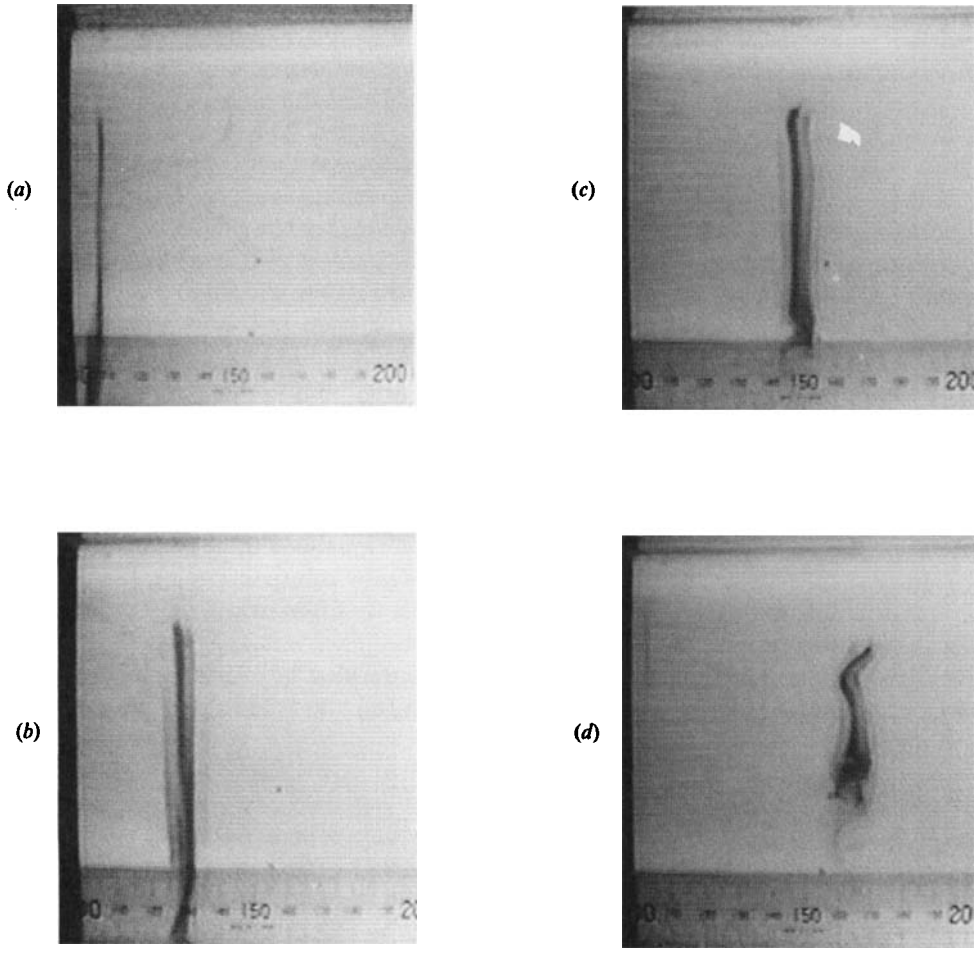

FIGURE 2. Behaviour of a vortex pair in still water. The vortex pair was ejected from a nozzle the edge of which is seen as a vertical thick black line at the let. The initial axis of the vortex pair was in the vertical direction. The time elapsed after the ejection is (*a*) 0.2 s, (*b*) 1.2 s, (*c*) 2.0 s and (*d*) 2.5 s.

represented. The flow was stratified by a simple procedure: (i) the channel was filled with tap water to 5 cm, the half-height of the channel; (ii) salt water was slowly slipped into the channel from underneath until the free surface was 9.5 cm high; (iii) the interface between the tap water and the salt water was stirred by hand for a few tens of seconds and left undisturbed for about fifteen minutes before the start of an experimental run. The salt water was prepared by adding 400 cm^3 of dry salt to 9090 cm^3 of tap water. After stirring, the density was expected to be about 1.05 near the bottom and unity at the free surface.

The blockage of flow in the test section by the plate amounted to 40%. This high blockage does not materially affect the basic patterns of interaction between a vortex ring and the shear-layer vortices. The main-stream velocity well upstream of the plate was 1.65 cm/s, whereas the flow at the middle of the gap between the edge of the plate and the opposite sidewall U'_∞ was accelerated to approximately 3.0 cm/s. The Reynolds number Re based on this velocity and the plate height was approximately 1000.

The shear-layer vortices were visualized by red food dye introduced near the front stagnation point of the plate. The density of the dye was carefully adjusted to be the same as that of the horizontal fluid layer where the vortices were visualized. The dye was convected towards the edge along the front face of the plate and subsequently shed downstream to visualize the separated shear layer. The previous discussion (§2.1) on vortex-like structures exhibited by the dye filament also applies to this case.

A vortex ring was generated by impulsively pushing out, by hand using a hypodermic syringe, a 'puff' of salt solution from a circular tube 0.5 cm in diameter. The volume of the puff was 2–3 cm^3 and this was pushed out in about 0.1 s. The vortex ring was made to travel in the horizontal layer where the shear-layer vortices were visualized. The density of the vortex ring was the same as that of the horizontal layer.

A drawback of the density stratification is that the vortex ring is compressed by the gravity force. The ratio of the inertial to gravitational forces of the vortex ring is of the order of the Froude number squared, i.e. F^2, where $F = V_{vr}/(2RN)$. Here V_{vr} is the translation velocity of the vortex ring, R is its radius and N denotes the Brunt–Väisälä frequency. In this experiment, typical values were $N \approx 2$–$3\ s^{-1}$, $2R \approx 0.8$ cm, $V_{vr} \approx 4$ cm/s, so that $F^2 \approx 6$–9. Thus the effect of gravitational force on the shear-layer vortices was expected to be relatively unimportant except for very weak vortex rings. Actually it was generally possible to differentiate the deformation due to the gravity from that due to the interaction.

Visualized patterns of the interaction were photographed by a motor-drive camera (4 frames/s) or by a 16 mm cine camera (24 frames/s).

3. The strength of the vortices

The patterns of the interaction between vortices may depend on many parameters such as their strength or circulation, shape, lengthscale, their relative position and attitude when they meet. We have assumed that the strength is the most important parameter in classifying the patterns, and this will be discussed in §4.

The circulation of a shear-layer vortex Γ_{sh} was estimated from

$$\Gamma_{sh} = \tfrac{1}{2} V_{sh}^2 \frac{l}{V_c}, \tag{1}$$

where V_{sh} is the velocity at the outer edge of the shear layer at separation, V_c is the convection velocity of the vortex and l denotes the average distance between two consecutive vortices. $\frac{1}{2}V_{sh}^2$ is the circulation shed per unit time from the separation line; l/V_c is the time interval of formation of the shear-layer vortices. V_{sh} and V_c were respectively taken as U_0 and $\frac{1}{2}U_0$, where U_0 was U_∞ in the vortex-pair experiment and U'_∞ in the vortex-ring experiment. The velocity V_{sh} can also be calculated in terms of the base pressure of the plate, but the base pressure was not measured in the present experiment. l was obtained from photographs like that shown in figure 3. Typical errors in obtaining V_{sh}, l and V_c were respectively estimated to be 5%, 10% and 5%; this results in an error of 25% for Γ_{sh}. Accordingly (1) gives only a rough measure of the circulation.

Since the strength of the shear-layer vortices increases with increasing longitudinal distance from the separation line, the circulation calculated from (1) gives an average value for two or three vortices such as shown in figure 3. Moreover, (1) is based on the assumption that all the vorticity shed downstream from the separation line finds its way into the shear-layer vortices.

The circulation Γ_{vp} of a vortex pair was calculated from the potential-flow formula

$$\Gamma_{vp} = 2\pi l_{vp} V_{vp}, \tag{2}$$

in terms of measured l_{vp}, the distance between the centre of the two vortices, and V_{vp}, their velocity of translation. The circulation of a real vortex pair decreases with increasing time (Maxworthy 1972), so this was determined from average values of l_{vp} and V_{vp} (estimated from flow-visualization photographs) from the time of its birth to the time when it started to interact with the shear-layer vortices. We appreciate that it is the value of circulation at the start of interaction that is essential in classifying interaction patterns. Obtaining this value, however, was difficult because it requires measuring the short distance travelled by a vortex pair in a brief interval of time. Errors in l_{vp} and V_{vp} were typically 10%, so that Γ_{vp} had an error of about 20%.

An estimation of the strength Γ_{vr} of a vortex ring was made on the basis of Saffman's (1970) formula for a viscous vortex ring

$$V_{vr} \approx \frac{\Gamma_{vr}}{4\pi R}\left[\log\left(\frac{8R}{\sigma}\right) - 0.558 + \ldots\right], \tag{3}$$

where V_{vr} is the velocity of translation, R is the radius of the ring and $\sigma\,(=(4\nu t)^{\frac{1}{2}}$, t being time) denotes the radius of the viscous core. The core radius was approximated as an average,

$$\overline{\sigma} = \frac{1}{T}\int_0^T \sigma \,\mathrm{d}t = \tfrac{2}{3}(4\nu t)^{\frac{1}{2}},$$

where T is the time at which R and V_{vr} were measured on a flow-visualization photograph. $\overline{\sigma}$ was typically of the order of 0.1 cm; this was not inconsistent with the flow-visualization photographs. For most of the vortex rings R was in the range 0.3–0.45 cm. We estimated an error of 20% for Γ_{vr}.

There is a circumferential instability mode of a vortex ring (Widnall & Sullivan 1973; Maxworthy 1977). In the present experiment, however, no such instability was observed, probably because the Reynolds number Γ_{vr}/ν was rather low, being in the range 30–180. It may be noted that the Reynolds number Γ_{vp}/ν for vortex pairs was in almost the same range, 10–160.

4. Results and discussion

4.1. *Vortex pair interacting with shear-layer vortices*

4.1.1. *Undisturbed shear-layer vortices*

Figure 3 shows an example of the shear-layer vortices undisturbed by external vortices. This photograph gives an idea of the lengthscale of the undisturbed shear-layer vortices. The strength Γ_{sh} estimated by (1) is probably the value for a vortex (in figure 3) located just above the nozzle.

In what follows, a vortex in a vortex pair whose circulation is of the same sign as the shear-layer vortices will be denoted by vortex P_1 while another vortex of the opposite sign will be called vortex P_2 as shown in figure 1.

4.1.2. *Vortex pairs stronger than the shear-layer vortices*

Figure 4 (plate 1) shows a pattern of interaction between a strong vortex pair and a shear-layer vortex ($\Gamma_{vp}/\Gamma_{sh} = 2.7 \pm 1.2$). The vortex P_2 starts to interact with a shear-layer vortex on its left in figure 4(*b*) and is seen to be temporarily compressed

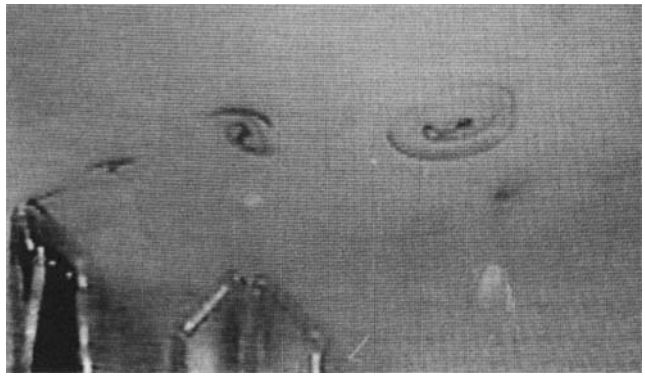

FIGURE 3. Rolled-up vortices in an undisturbed shear layer. The distance between the front of the plate and the centre of the nozzle is about 0.75 times the plate height h. Flow is from left to right. $U_\infty = 2.0$ cm/s and $U_\infty h/\nu = 600$.

flat in figure 4(*c*). P_1, on the other hand, behaves rather independently and is diffused after becoming three-dimensional, as seen in figure 4(*e*).

Figure 4(*f*) shows the flow pattern at some time after the interaction. An interesting feature is that an extremely large shear-layer vortex is formed just downstream of the edge of the plate. The vortex is large in the sense that such a lengthscale was not attained at the same longitudinal position in the undisturbed shear layer. During the interaction the vorticity shed from the separation line was accumulated between the edge and the interaction region; this led to the formation of the large vortex.

Other patterns were also observed depending on a difference in phase when the vortices met, although they are not shown here. Typical patterns were: (i) a vortex pair interacting with a shear-layer vortex on the right; (ii) a vortex pair striking head-on a shear-layer vortex; and (iii) a vortex pair passing through the middle of two consecutive shear-layer vortices.

These patterns are characterized by the fact that the vortex pairs generally behaved as a single unit during the interaction even though the two constituent vortices experienced a considerable deformation and the distance between their centres was considerably increased. These patterns were observed when the circulations Γ_{vp} and Γ_{sh} were correlated as in figure 5. Eighty per cent of the data fall in a parameter space $\Gamma_{vp}/\Gamma_{sh} = 1.4 \pm 0.5$. This large scatter was caused partly by the large uncertainties in estimating the circulations and partly by the difficulty in discriminating between the interaction patterns.

4.1.3. *Vortex pairs of similar strength as the shear-layer vortices*

Figure 6 (plate 2) shows an interaction pattern where the vortex pair is of strength defined by $\Gamma_{vp}/\Gamma_{sh} = 0.70 \pm 0.28$. In figure 6(*b*), the vortex pair is moving towards the middle of two amalgamating shear-layer vortices. The vortex P_1 is entrained into the amalgamating vortices to form a large vortex as seen in figures 6(*d–f*).

The vortex P_2, on the other hand, forms a new vortex pair with another shear-layer vortex growing at its left. The formation of the new vortex pair is manifested by a downward motion of the two vortices seen in figures 6(*e–g*); further downward motion is prohibited by the nozzle.

An important feature of this pattern is the splitting of the original vortex pair; that is the distance between P_1 and P_2 is increased enormously by the interaction.

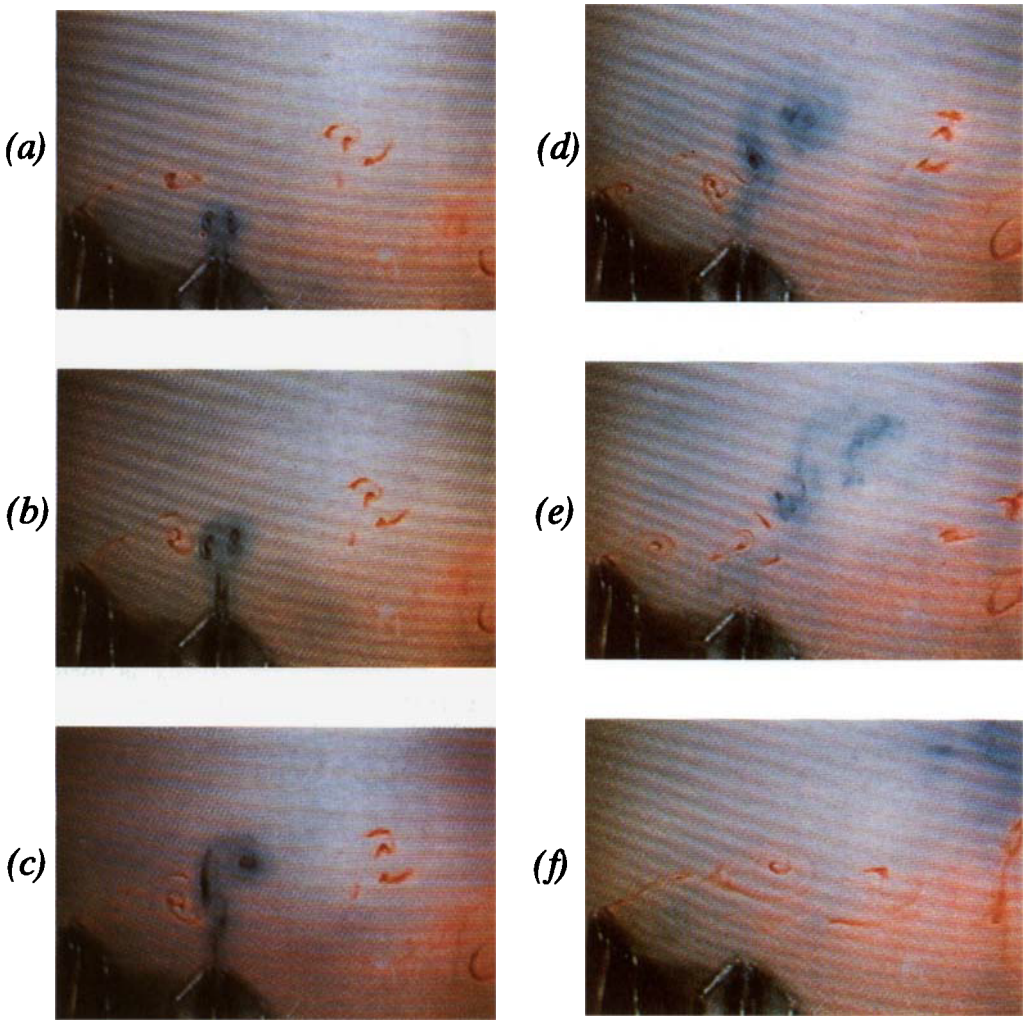

FIGURE 4. Interaction between a strong vortex pair and a shear-layer vortex to its left. Flow is from left to right. U_∞ = 2.0 cm/s, Γ_{vp} = 16 cm^2/s and Γ_{sh} = 5.9 cm^2/s. The time interval between two consecutive photographs is (*a–c*) 0.3 s, (*c–d*) 0.5 s, (*d–e*) 1.0 s, and (*e–f*) 2.0 s.

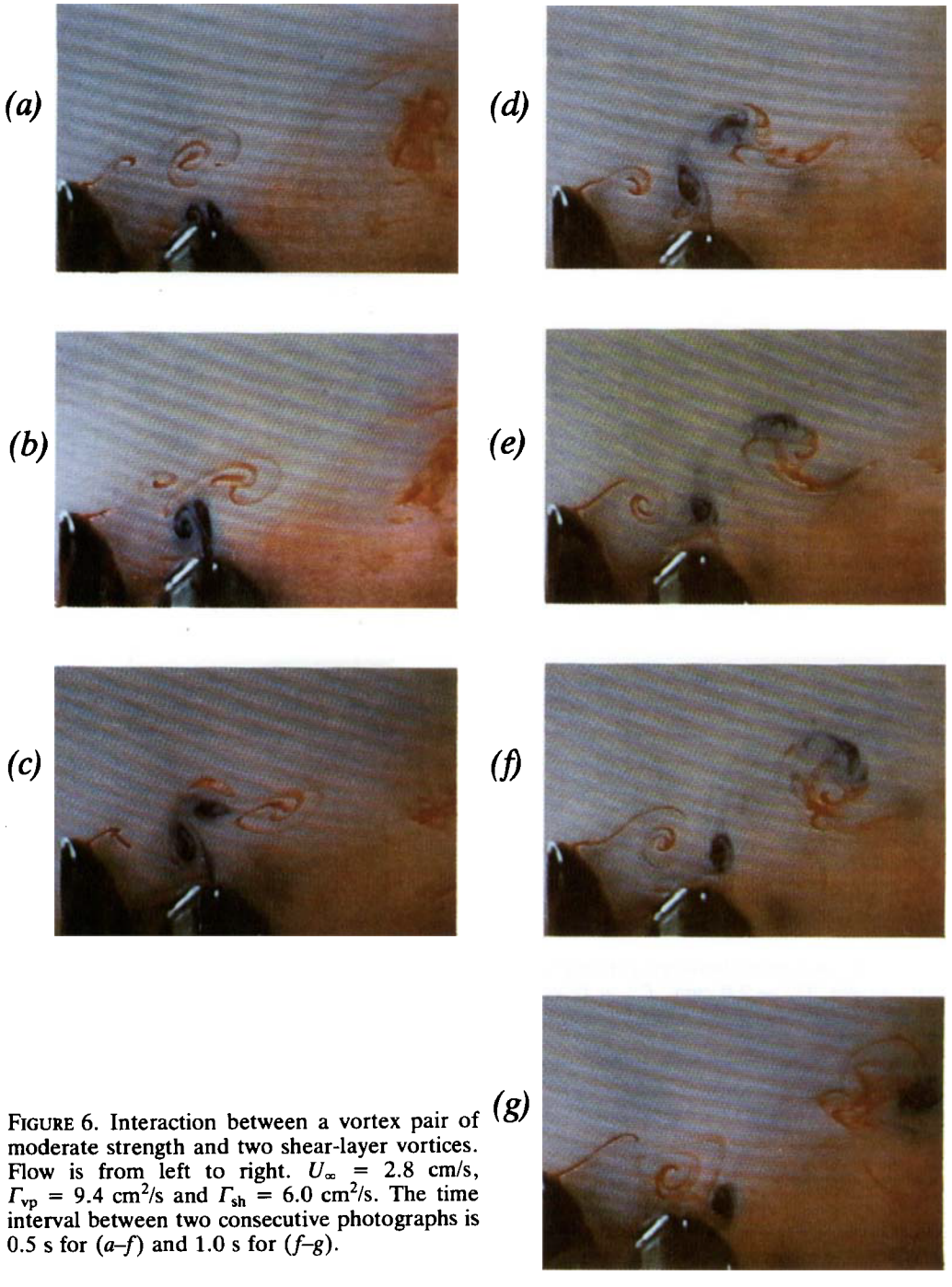

FIGURE 6. Interaction between a vortex pair of moderate strength and two shear-layer vortices. Flow is from left to right. U_∞ = 2.8 cm/s, Γ_{vp} = 9.4 cm^2/s and Γ_{sh} = 6.0 cm^2/s. The time interval between two consecutive photographs is 0.5 s for (*a–f*) and 1.0 s for (*f–g*).

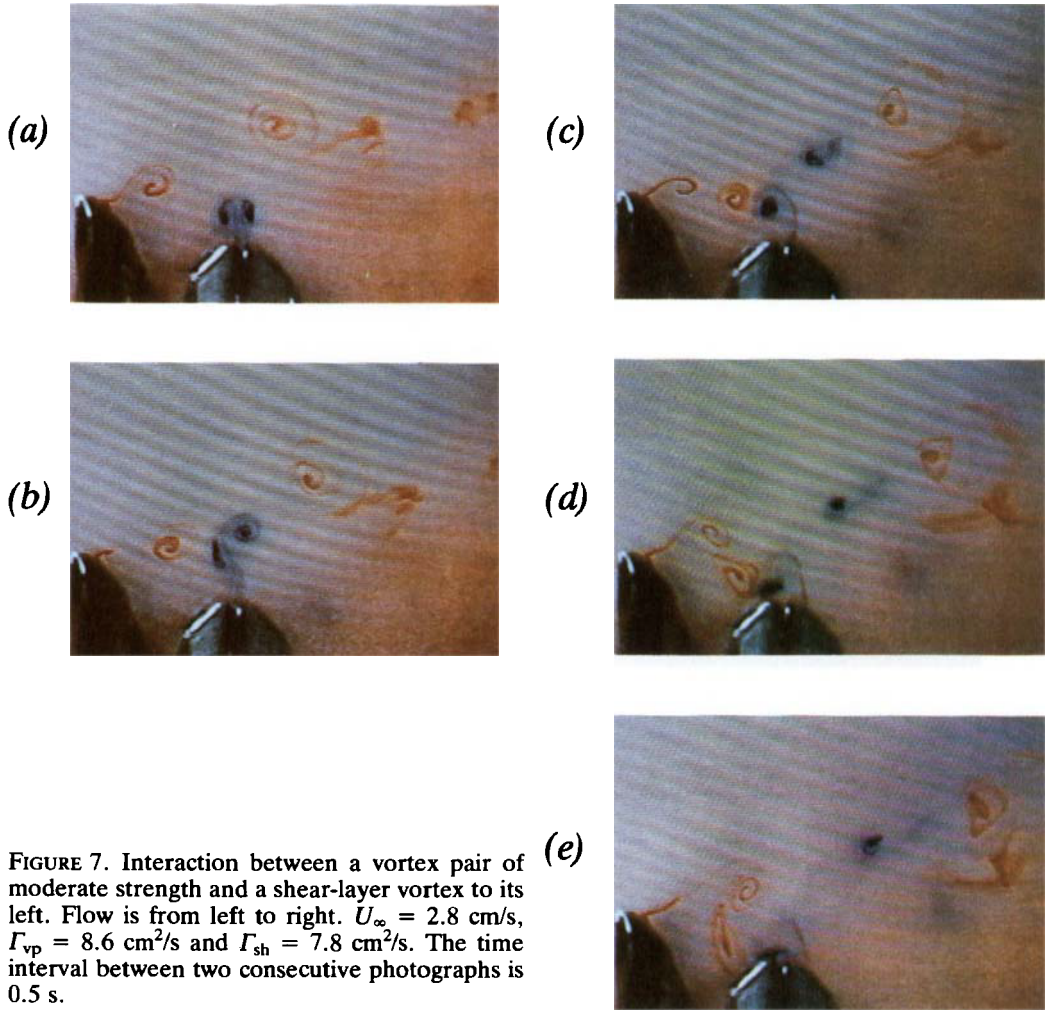

FIGURE 7. Interaction between a vortex pair of moderate strength and a shear-layer vortex to its left. Flow is from left to right. U_∞ = 2.8 cm/s, Γ_{vp} = 8.6 cm^2/s and Γ_{sh} = 7.8 cm^2/s. The time interval between two consecutive photographs is 0.5 s.

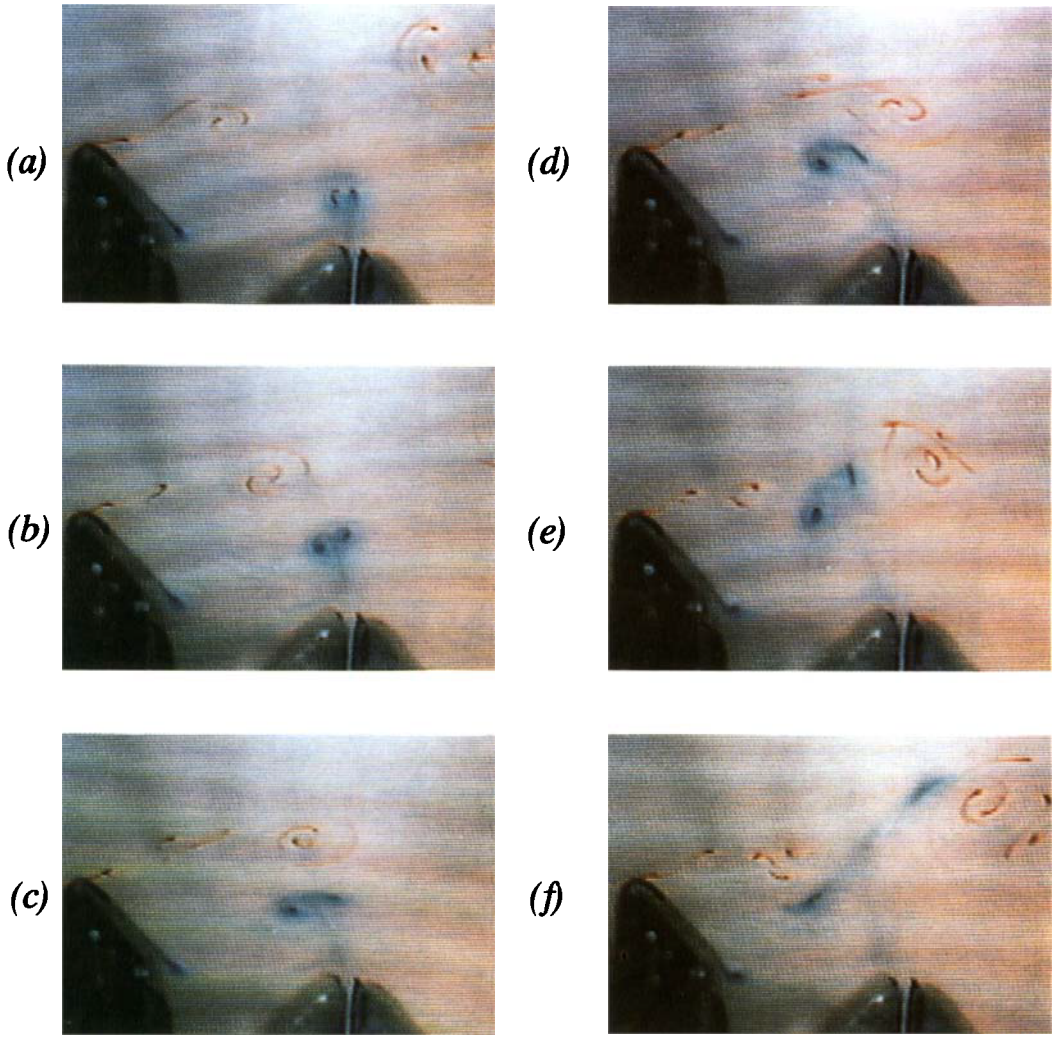

FIGURE 9. Interaction between a weak vortex pair and a few shear-layer vortices. Flow is from left to right. $U_\infty = 2.3$ cm/s, $\Gamma_{vp} = 1.5\,\text{cm}^2/\text{s}$ and $\Gamma_{sh} = 5.8\,\text{cm}^2/\text{s}$. The time interval between two consecutive photographs is 0.5 s.

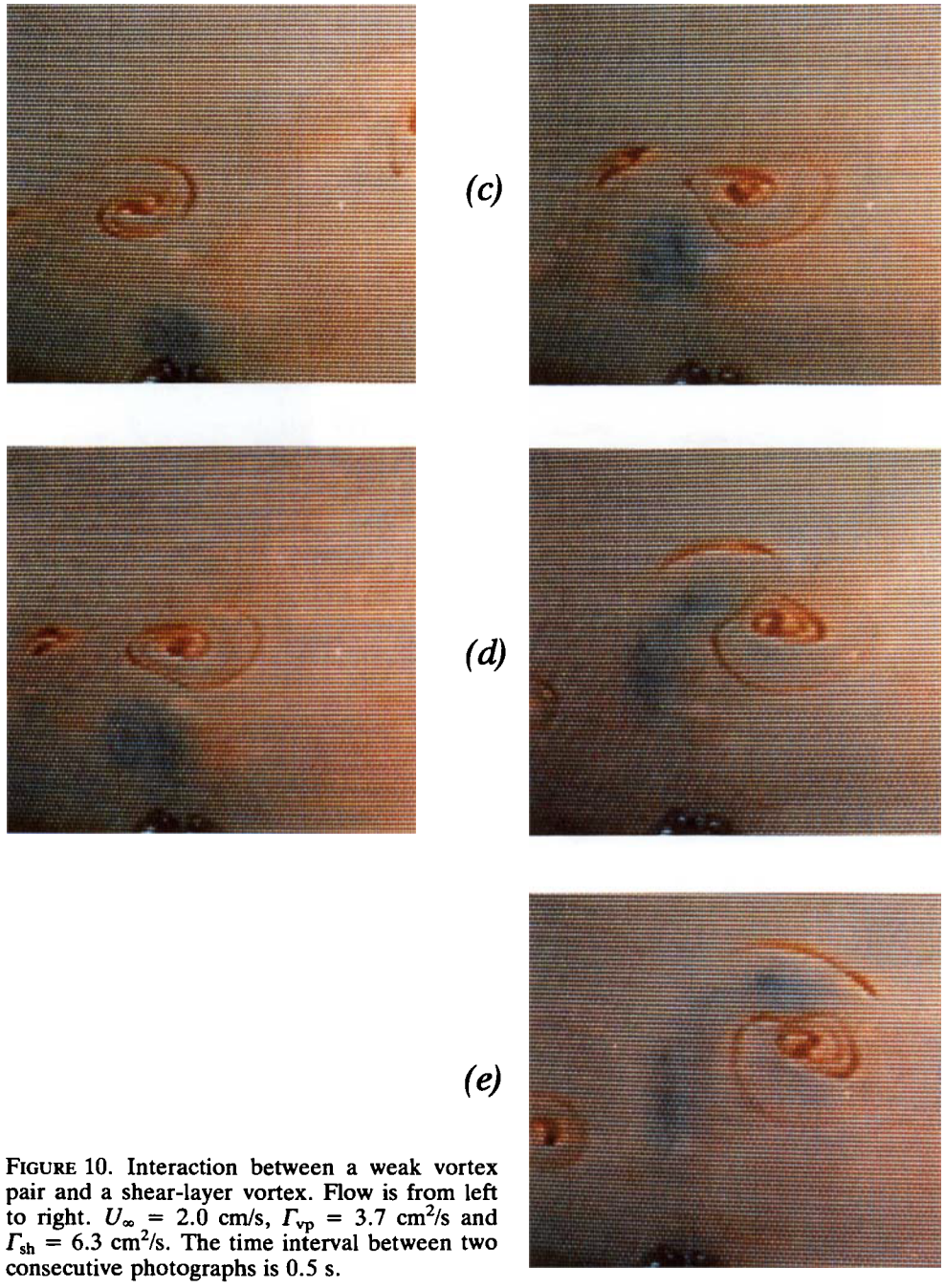

FIGURE 10. Interaction between a weak vortex pair and a shear-layer vortex. Flow is from left to right. U_∞ = 2.0 cm/s, Γ_{vp} = 3.7 cm^2/s and Γ_{sh} = 6.3 cm^2/s. The time interval between two consecutive photographs is 0.5 s.

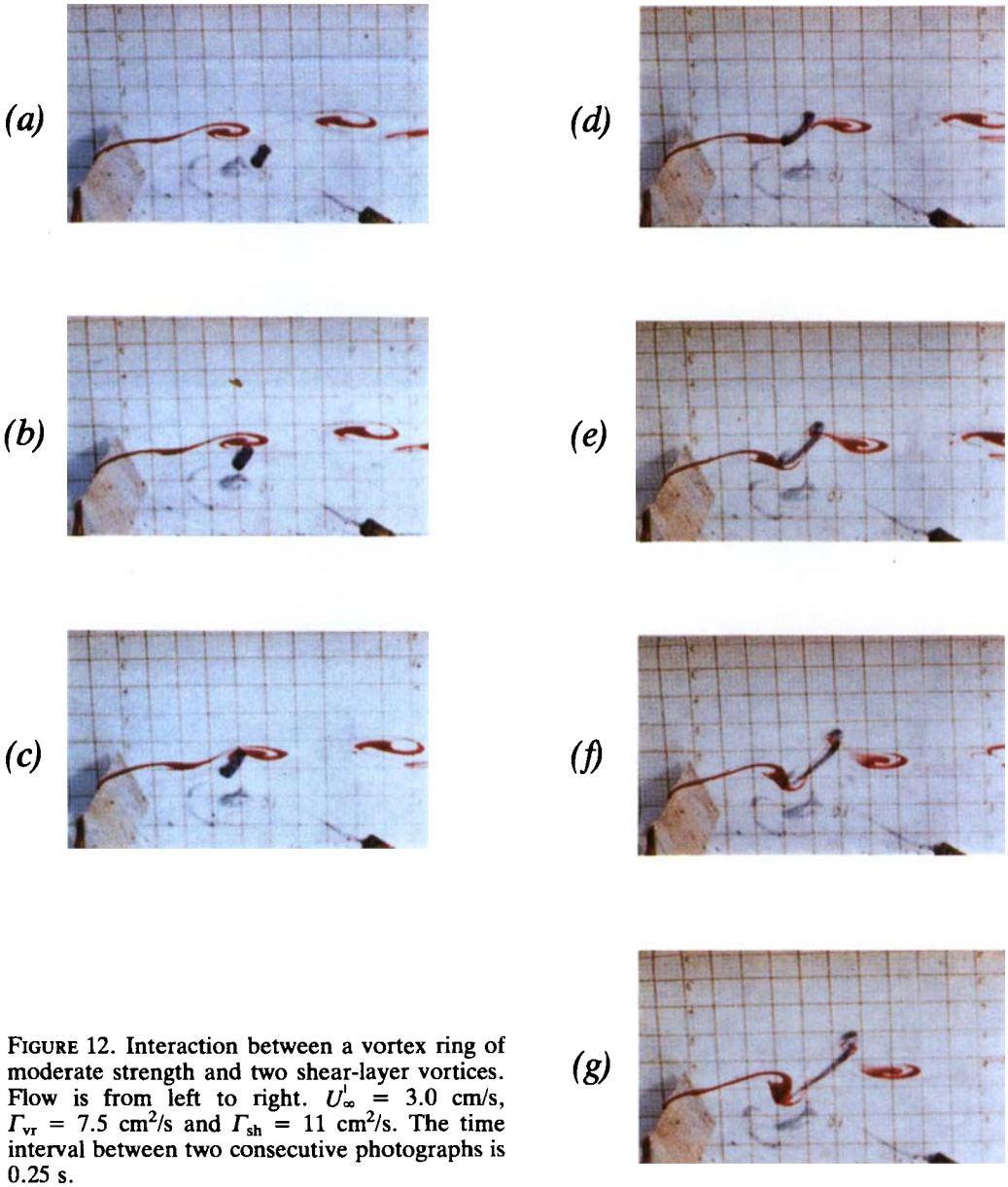

FIGURE 12. Interaction between a vortex ring of moderate strength and two shear-layer vortices. Flow is from left to right. $U_\infty^{\downarrow}$ = 3.0 cm/s, Γ_{vr} = 7.5 cm^2/s and Γ_{sh} = 11 cm^2/s. The time interval between two consecutive photographs is 0.25 s.

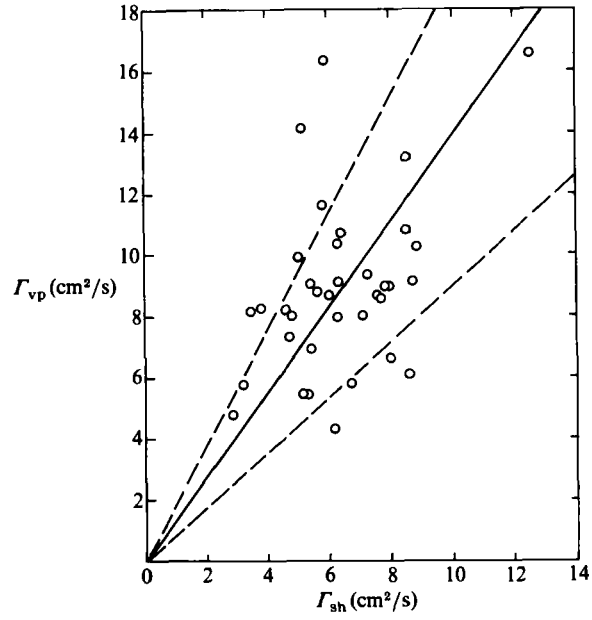

FIGURE 5. Correlation between the strength of a vortex pair Γ_{vp} and that of a shear-layer vortex Γ_{sh} for patterns similar to figure 4: ——, $\Gamma_{vp}/\Gamma_{sh} = 1.4$; – – –, $\Gamma_{vp}/\Gamma_{sh} = 1.4 \pm 0.5$.

We also note the marked increase in the diameter of the shear-layer vortex that forms a pair with the vortex P_2.

In figure 7(*a*) (plate 3) a vortex pair interacts with a shear-layer vortex to its left ($\Gamma_{vp}/\Gamma_{sh} = 1.56 \pm 0.62$). A temporary compression of P_2 is observed in figure 7(*b*). As in figure 6, P_2 forms a new vortex pair with the shear-layer vortex. This shear-layer vortex eventually attains a large scale by amalgamating with the next shear-layer vortex as seen in figures 7(*d–e*). On the other hand, P_1 eventually amalgamates with the rightmost shear-layer vortex in figure 7(*e*). If a vortex pair of this strength directly strikes a shear-layer vortex, a pattern similar to figure 7 is observed.

The above patterns are characterized by the splitting of the vortex pairs and the resulting formation of two large shear-layer vortices. Figure 8 shows how the circulations Γ_{vp} and Γ_{sh} are correlated when these interaction patterns appear. 90% of the data fall in a parameter space $\Gamma_{vp}/\Gamma_{sh} = 1.0 \pm 0.5$.

4.1.4. *Vortex pairs weaker than the shear-layer vortices*

Figure 9 (plate 4) shows a pattern of interaction in this category where $\Gamma_{vp}/\Gamma_{sh} = 0.25 \pm 0.10$. In figure 9(*a*) a vortex pair is moving towards the middle of the two shear-layer vortices. The momentum of the vortex pair is so low that it is rotated around a shear-layer vortex as seen in figures 9(*b–d*). In figure 9(*e*), the vortex pair is approaching a saddle between two consecutive shear-layer vortices and experiences a sudden split, see figure 9(*f*). Eventually the vortices P_1 and P_2 are independently entrained into the shear-layer vortices. The shear-layer vortices themselves seem to be little influenced by the vortex pair. Another example is shown in figure 10 (plate 5), where a vortex pair is entrained into two amalgamating shear-layer vortices.

Patterns of this category are characterized by the passive deformation of the vortex pair around the shear-layer vortices; the circulations Γ_{vp} and Γ_{sh} are correlated as shown in figure 11 : 80% of the data fall in the range $\Gamma_{vp}/\Gamma_{sh} = 0.5 \pm 0.3$.

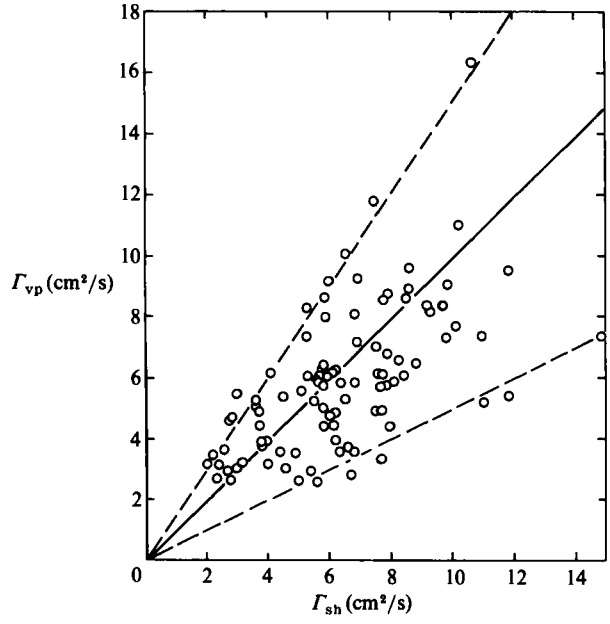

FIGURE 8. Correlation between the strength of a vortex pair Γ_{vp} and that of shear-layer vortices Γ_{sh} for patterns similar to figures 6 and 7: ----, $\Gamma_{vp}/\Gamma_{sh} = 1.0$; ---, $\Gamma_{vp}/\Gamma_{sh} = 1.0 \pm 0.5$.

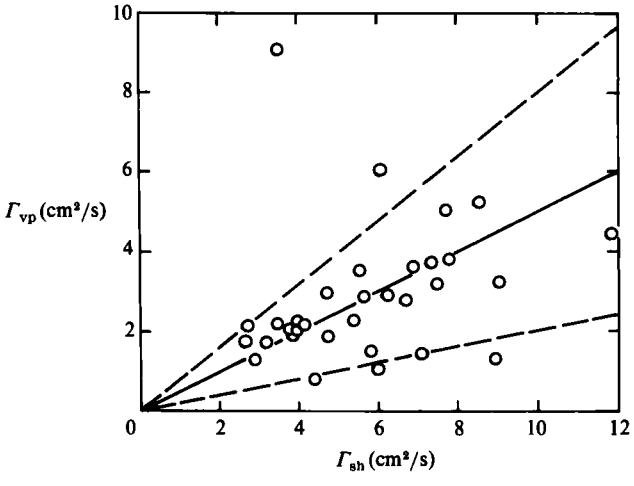

FIGURE 11. Correlation between the strength of a vortex pair Γ_{vp} and that of a shear-layer vortex Γ_{sh} for patterns similar to figures 9 and 10: ——, $\Gamma_{vp}/\Gamma_{sh} = 0.5$; ---, $\Gamma_{vp}/\Gamma_{sh} = 0.5 \pm 0.3$.

4.2. *Vortex ring interacting with the shear-layer vortices*

Although a number of observations were made of interaction between single vortex rings and shear-layer vortices, only one typical set of observations are presented: figure 12 (plate 6) shows a vortex ring interacting with a shear-layer vortex at its left, when $\Gamma_{vr}/\Gamma_{sh} = 0.7$. The vortex ring is seen to experience an enormous stretching; its ends were separately entrained into nearby shear-layer vortices, see figures 12(*e–g*). A comparison of this pattern with figures 6 and 7 suggests that the

stretching corresponds qualitatively to the splitting of a vortex pair. It may be noted, however, that this is the case only when a vortex ring travels in the plane normal to the flow, which is perpendicular to the vortices in the shear layer.

On the other hand, the leftmost shear-layer vortex, which has entrained the upstream end of the vortex ring, seems to be somewhat larger than the undisturbed shear-layer vortex observed at the same longitudinal position, see figures 12(*a*, *g*). This stretching and the increase in the lengthscale of the shear-layer vortices was typical of interaction when Γ_{vr}/Γ_{sh} was of the order of unity.

Weaker vortex rings were stretched and eventually entrained into nearby shear-layer vortices, without affecting the latter to any significant extent. This is similar to figures 9 and 10 for a vortex pair. On the other hand, stronger vortex rings did not generally disintegrate; they simply dragged with them any shear-layer vortex in their path.†

5. A numerical model

In order to interpret the motion of a vortex pair and the shear-layer vortices during the interaction, a model calculation was performed. We assume that the motion of the vortices is approximated by that of inviscid rectilinear vortices, at least in an initial phase of the interaction. Accordingly, the shear-layer vortices were represented by a large number of rectilinear vortices (with circulation Γ_{sh}) arranged with a constant distance between them in the longitudinal direction. The distance between two consecutive vortices is denoted by l. The total number of rectilinear vortices n was chosen as 50, a choice justified by the fact that no discernible differences in calculated results were observed for $n = 50$ and 100. Of the 50 vortices, the four central vortices were allowed to move when a vortex pair was introduced into their vicinity; other vortices were fixed.

In view of figures 4(*a*), 6(*a*) and 7(*a*), the pair vortices were initially separated by a distance $0.2l$ in the longitudinal direction and located $0.5l$ below the vortex array. The initial longitudinal position of their centres was systematically changed between the innermost two free vortices. Also, the ratio Γ_{vp}/Γ_{sh} was chosen as 1.4, 1.0 and 0.5 in view of the results described in §4.1.

The calculated motions of the vortices are shown with reference to coordinates moving with the modelled shear-layer vortices, whereas in the experiment they were observed in a stationary frame. This difference, however, poses no serious difficulty in comparing the calculated and observed patterns.

A typical example for $\Gamma_{vp}/\Gamma_{sh} = 1.4$ is shown in figure 13, in which a vortex pair interacts with a shear-layer vortex to its left. This vortex tends to rotate around the vortex P_2, which in turn pauses near the shear-layer vortex. The distance between P_1 and P_2 slightly increases during the pause of P_2. This pattern approximately corresponds to the motion of the centres of mass of the dye of vortices P_1 and P_2 in figures 4(*b–d*). For vortices with finite core sizes, the interaction between P_2 and the shear-layer vortex causes the vortex cores to be stretched and eventually torn apart, a striking feature of figures 4(*b–d*).

Figure 14 shows the pattern when all the vortices have the same strength, i.e. $\Gamma_{vp}/\Gamma_{sh} = 1.0$, which approximately corresponds to the situation shown in figures 6 and 7. When a vortex pair meets a shear-layer vortex on its left, the latter forms a new vortex pair with a vortex P_2, and moves in a straight path towards the bottom left of the figure with velocity of the same order as that of the original vortex pair.

† These data are available from Dr Kiya on request.

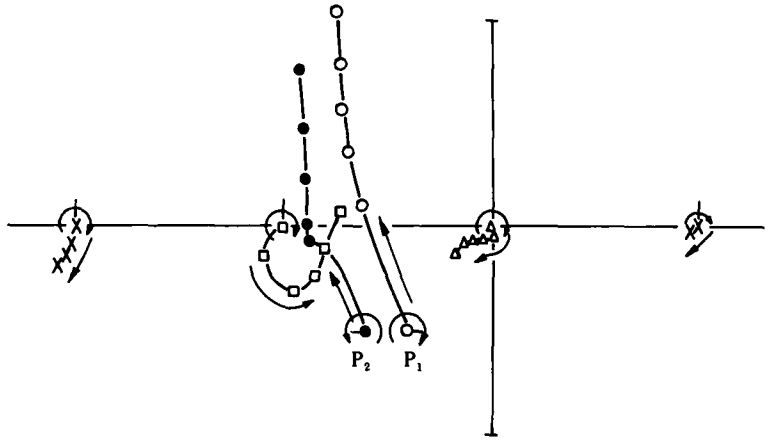

FIGURE 13. Calculated pattern of interaction between a vortex pair and shear-layer vortices for $\Gamma_{vp}/\Gamma_{sh} = 1.4$. Symbols show the positions of vortices at constant times after the development of the vortex pair. Horizontal flags show the initial position of vortex pair, whereas vertical flags denote the initial longitudinal position of shear-layer vortices.

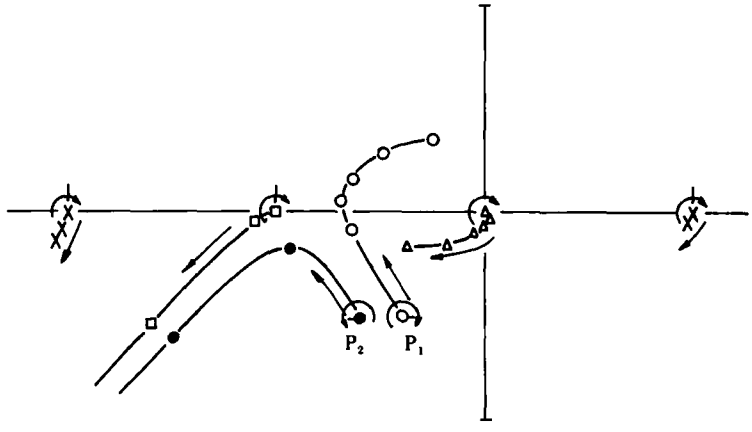

FIGURE 14. Calculated pattern of interaction between a vortex pair and shear-layer vortices for $\Gamma_{vp}/\Gamma_{sh} = 1.0$. Symbols as in figure 13.

On the other hand, P_1 and another shear-layer vortex at the right rotate around each other with a radius of about $\frac{1}{4}l$; this suggests the amalgamation of the two vortices. These features correspond well with the experimental patterns of figures 6 and 7 (taking into account the differences between the experimental and numerical observing coordinate frames).

A typical interaction of a weak vortex pair and an effectively isolated shear-layer vortex, where $\Gamma_{vp}/\Gamma_{sh} = 0.5$, is shown in figure 15. The effect of the other shear-layer vortices on the interaction is very weak. The vortex pair initially moving upwads is deflected and rotates around the shear-layer vortex, before leaving in a different direction. This pattern may correspond to the rotation of a vortex pair around a shear-layer vortex shown in figure 10. In that figure, the large shear-layer vortex is already merging with another shear-layer vortex, so the vortex pair is readily engulfed into the merging process.

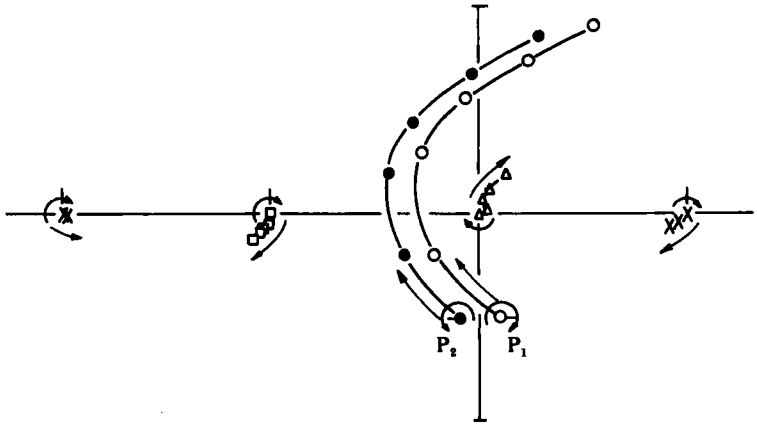

FIGURE 15. Calculated pattern of interaction between a vortex pair and shear-layer vortices for $\Gamma_{vp}/\Gamma_{sh} = 0.5$. Symbols as in figure 13.

Figure 16 demonstrates a different pattern for $\Gamma_{vp}/\Gamma_{sh} = 0.5$ in which a vortex pair is split by two shear-layer vortices. At an early stage the vortex pair is rotated around a shear-layer vortex on its right, which deflects it towards the shear-layer vortex on its left. When the vortex pair reaches the middle of the shear-layer vortices, P_2 forms a vortex-pair-like structure with the shear-layer vortex on the left, and rotates on a path with a radius of about $4l_{vp}$. (This radius of curvature is of order $l_{vp}\Gamma_{sh}^2/((\Gamma_{sh}-\Gamma_{vp})\Gamma_{vp})$.) This results in an enormous increase in the distance between the vortices P_1 and P_2. At the same time, P_1 rotates around the shear-layer vortex to the right. This pattern approximately corresponds to the successive photographs of figure 9.

6. Concluding remarks

The vortex-pairing mechanism in free-mixing layers has been established by previous research to be the major mechanism causing the growth in their thickness with downwind distance. Such vortex pairing contributes to the aerodynamic-noise generation and to the production of Reynolds shearing stress. Free-stream turbulence is likely to affect this process. It is also likely to distort the individual shear-layer vortices. This might trigger the kind of instability considered by Widnall & Sullivan (1973) if the wavelength of any induced spanwise waviness of the vortices is large compared with the diameter of their cores. But this kind of interaction was not considered here.

The present experiment demonstrated that the vortex pairing can be disturbed by individual vortex pairs and rings propelled towards the shear-layer vortices. Although patterns of the interaction may depend on many parameters, the strength was found to serve as a rough measure to classify them into three regimes. The interaction is expected to increase the growth rate and the turbulence level in the free-mixing layers (Pui & Gartshore 1979). This also suggests that they can be manipulated by such external vortices.

Three mechanisms have been suggested for the free-stream turbulence effects on shear layers: (i) direct interaction of free-stream vortices with coherent vortices in shear layers; (ii) a weak, but still direct, effect of free-stream vortices, in which they may affect the coalescence and tearing of vortices in shear layers; (iii) free-stream vortices inducing irrotational fluctuations and thence the growth of rotational

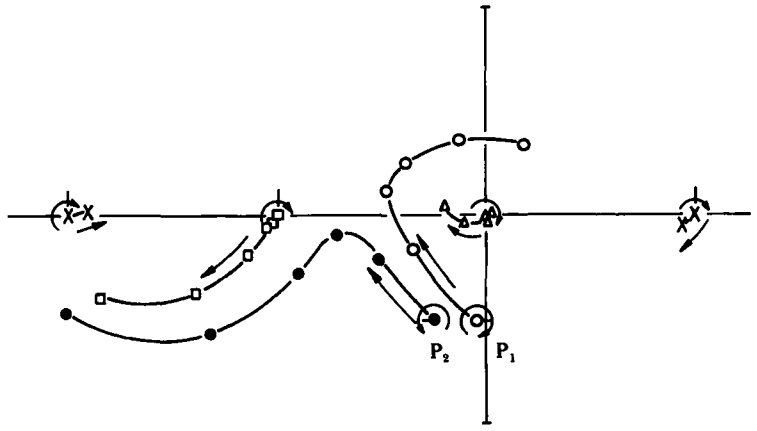

FIGURE 16. Calculated pattern of interaction between a vortex pair and shear-layer vortices for $\Gamma_{vp}/\Gamma_{sh} = 0.5$. Symbols as in figure 13.

fluctuations in the mean velocity gradient of shear layers (Gartshore, Durbin & Hunt 1983). The present study is addressed to the first and second effects.

It is hoped that this study has disclosed some fundamental aspects of the vortex interaction, which may help generally to understand the free-stream turbulence effects on shear flows. This work can be extended to a mixing layer being excited artificially so that the phase of the mixing-layer vortices, relative to that of the (power-propelled) vortex injection, would be controlled (this suggestion was made by a referee).

The experimental work described in §4.2 was done while M.K. was a visitor at the Department of Applied Mathematics and Theoretical Physics, the University of Cambridge, UK, supported by the Ministry of Education, Science and Culture of Japan. Thanks are due to Mr E. P. Sutton, Dr R. E. Britter, Dr J. C. Mumford and Dr M. Savill for their valuable discussions during the experiment and the writing up, and to Mr B. Peck and to Mr Nesbit of the University Engineering Department for their assistance. The authors are grateful to Mr T. Sato for performing the numerical culation described in §5 and to the referees for their helpful comments which have led to an improved presentation of the paper.

REFERENCES

AREF, H. 1983 Integrable, chaotic, and turbulent vortex motion in two-dimensional flows. *Ann. Rev. Fluid Mech.* **15**, 345–389.

BATCHELOR, G. K. 1967 *An Introduction to Fluid Dynamics*. Cambridge University Press.

BRADSHAW, P. 1974 Effects of free-stream turbulence on turbulent shear layers. *Imperial College Aero Rep.* 74–10.

BRADSHAW, P. 1977 Interacting shear layers in turbomachines and diffusers. In *Turbulence in Internal Flows: Turbomachinery and Other Engineering Applications* (ed. S. N. B. Murthy), pp. 35–65. Hemisphere.

BRIGHTON, P. W. M. 1977 Boundary layers and stratified flows past obstacles. Ph.D. thesis, University of Cambridge.

CASTRO, I. P. 1984 Effects of free-stream turbulence on low Reynolds number boundary layers. *Trans. ASME* I: *J. Fluids Engng* **106**, 298–306.

CHANDRSUDA, C., MEHTA, R. D., WEIR, A. D. & BRADSHAW, P. 1978 Effect of free-stream turbulence on large structure in turbulent mixing layers. *J. Fluid Mech.* **85**, 693–704.

CROW, S. C. 1970 Stability theory for a pair of trailing vortices. *AIAA J.* **8**, 2172–2179.

FALCO, R. E. 1977 Coherent motions in the outer region of turbulent boundary layers. *Phys. Fluids* **20**, S124–S132.

GARTSHORE, I. S., DURBIN, P. A. & HUNT, J. C. R. 1983 The production of turbulent stress in a shear flow by irrotational fluctuations. *J. Fluid Mech.* **137**, 307–329.

HANCOCK, P. E. & BRADSHAW, P. 1983 The effect of free-stream turbulence on turbulent boundary layers. *Trans. ASME* I: *J. Fluids Engng* **105**, 284–289.

HEAD, M. R. & BANDYOPADHYAY, P. 1983 New aspects of turbulent boundary layer structure. *J. Fluid Mech.* **107**, 297–338.

MAXWORTHY, T. 1972 The structure and stability of vortex rings. *J. Fluid Mech.* **51**, 15–32.

MAXWORTHY, T. 1977 Some experimental studies of vortex rings. *J. Fluid Mech.* **81**, 465–495.

ODELL, G. M. & KOVASZNAY, L. S. G. 1971 A new type of water channel with density stratification. *J. Fluid Mech.* **50**, 535–543.

OGUCHI, H. & INOUE, O. 1984 Mixing layer produced by a screen and its dependence on initial conditions. *J. Fluid Mech.* **142**, 217–231.

OVERMAN, E. A. & ZABUSKY, N. J. 1982 Evolution and merger of isolated vortex structures. *Phys. Fluids* **25**, 1297–1305.

PERRY, A. E. & LIM, T. T. 1978 Coherent structures in coflowing jets and wakes. *J. Fluid Mech.* **88**, 451–463.

PUI, N. K. & GARTSHORE, I. S. 1979 Measurements of the growth rate and structure in plane turbulent mixing layers. *J. Fluid Mech.* **91**, 111–130.

SAFFMAN, P. G. 1970 The velocity of viscous vortex rings. *Stud. Appl. Math.* **49**, 371–380.

SYMES, C. R. & FINK, L. E. 1977 Effects of external turbulence upon the flow past cylinders. In *Structure and Mechanism of Turbulence I* (ed. H. Fiedler), pp. 86–102. Springer.

TAMURA, H., KIYA, M. & ARIE, M. 1984 Vortex shedding from a two-dimensional blunt trailing edge with unequal external free-stream velocities. *Bull. JSME* **27**, 1866–1872.

TATSUNO, M. & HONJI, H. 1977 Two pairs of rectilinear vortices. *J. Phys. Soc. Japan* **42**, 361–362.

WIDNALL, S. E. & SULLIVAN, D. B. 1973 On the stability of vortex rings. *Proc. R. Soc. Lond.* A **332**, 335–353.

WINANT, C. D. & BROWAND, F. K. 1974 Vortex pairing: the mechanism of turbulent mixing-layer growth at moderate Reynolds number. *J. Fluid Mech.* **63**, 237–255.

WYGNANSKI, I., OSTER, D., FIEDLER, H. & DZIOMBA, B. 1979 On the preserverance of a quasi-two-dimensional eddy-structure in a turbulent mixing layer. *J. Fluid Mech.* **93**, 325–335.

YAMADA, H. & MATSUI, T. 1979 Mutual slip-through of a pair of vortex rings. *Phys. Fluids* **22**, 1245–1249.

ZABUSKY, M. D., HUGHES, M. H. & ROBERTS, K. V. 1979 Contour dynamics for the Euler equations in two dimensions. *J. Comp. Phys.* **30**, 96–106.